IEEE Access
Multidisciplinary | Rapid Review | Open Access Journal

Received December 14, 2018, accepted December 23, 2018, date of current version February 4, 2019.

Digital Object Identifier 10.1109/ACCESS.2018.2890170

Simultaneous Chaos Time-Delay Signature Cancellation and Bandwidth Enhancement in Cascade-Coupled Semiconductor Ring Lasers

PENGHUA MU[1], (Member, IEEE), PENGFEI HE[1], AND NIANQIANG LI[2], (Member, IEEE)
[1]School of Opto-electronic Information Science and Technology, Yantai University, Shandong 264003, China
[2]Microwave Photonic Research Laboratory, School of Electrical Engineering and Computer Science, University of Ottawa, Ottawa, ON K1N 6N5, Canada

Corresponding author: Nianqiang Li (wan_103301@163.com)

This work was supported by the National Nature Science Fund of China under Grant 61202399.

ABSTRACT Optics chaos has been widely studied and its various applications have also been demonstrated in recent years. To improve the performance of chaos-based applications, several properties of the chaotic signals should be evaluated and enhanced accordingly. In this paper, we consider a chaotic system consisting of three cascade-coupled semiconductor ring lasers (SRLs), where the master SRL is subjected to conventional (parallel) optical feedback, while its output is injected to the intermediate SRL and further to the slave SRL. We focus on the time-delay signature (TDS) and bandwidth of the generated chaos and demonstrate the possibility of the simultaneous realization of TDS elimination and bandwidth enhancement in the parameter space of the injection strength against the frequency detuning. In addition, a proof-of-concept test of randomness is carried out, and it demonstrates that the chaotic properties could be greatly enhanced by the proposed cascade-coupling scheme compared with a single SRL with feedback and thus is suitable for use in high-speed random number generation.

INDEX TERMS Nonlinear dynamics, optical chaos, semiconductor ring laser, time-delay signature, bandwidth.

I. INTRODUCTION

Laser chaos has attracted widespread attention since its potential applications to chaos-based communications [1]–[5], ultrafast random generation (RNG) [6]–[9], compressive sensing [10], neuro-inspired signal processing [11]–[13] and chaotic radar/LIDAR [14]. Conventional semiconductor lasers usually yield simple, continuous wave when isolated from any kind of perturbations. On the contrary, they are destabilized by either feedback or injection forcing and rich dynamics can be expected in these laser systems in the presence of additional degrees of freedom [15]–[20]. Among these, a semiconductor laser subjected to optical feedback has been widely employed for chaos generation due to its simplicity and ease of implementation. However, the resulting chaos exhibits strong correlation at the location of the time lag corresponding to the feedback length, which has been termed time-delay signature (TDS) in the literature. Such autocorrelation properties could be easily extracted and haven been investigated in many published papers [21]–[25]. It is believed that TDS degrades the performance of chaos-based applications, for example, TDS leakage not only is a serious threat to the security of secure communications [24], but also hinders the pass of randomness tests in RNG [6].

The suppression of the unwanted TDS is the critical challenge that is being faced in the field of chaos-based applications where the chaotic source is generated by an external-cavity semiconductor laser (ECSL). In recent years, various schemes have been proposed to weaken or even eliminate TDS [25]–[35]. For example, the TDS can be greatly suppressed by incorporating multiple feedback loops into the laser system, considering complex feedback schemes, or receiving feedback from another active device (e.g., another laser) [25]–[28]. However, in these cases, the bandwidth is limited to the range of several GHz, which cannot meet the requirement of the modern applications.

On the contrary, it has been found that an optical injection scheme allows the simultaneous achievement of TDS suppression and bandwidth enhancement, which makes it a tempting option. This can be realized in the

conventional semiconductor lasers as well as in other novel laser architectures, e.g., vertical-cavity surface-emitting semiconductor lasers (VCSELs) [29]–[33]. However, the parameter region for simultaneously achieving these goals is very narrow, which is not suitable for practical applications. Later on, researchers have proposed a three cascade-coupled laser configuration, which enhances the chaotic dynamics in much wider regions of the injection strength against the frequency detuning [34]–[38]. Especially, high quality RNG whose maximum generation rate reaches 1.2 Tb/s has been realized using three-cascaded semiconductor lasers, which benefits from the TDS elimination and bandwidth enhancement [38]. Very recently, some modified injection schemes for TDS suppression have also been proposed, where the injected medium is not limited to a laser [39]–[42]. The generation of broadband chaos with perfect TDS suppression becomes possible in these schemes. Moreover, it is worth noting that chaos TDS can also be cancelled by using advanced detection techniques including optical and electrical heterodyne [43], [44]. Despite the large amount of publications in this topic, it is still of interest to generate broadband chaos with no obvious TDS in alternative systems due to its potential use in secure communications and RNG.

Unlike any lasers mentioned above, a semiconductor ring laser (SRL) supports clockwise (CW) and counter clockwise (CCW) propagation modes in a cavity with a circular geometry [45]–[51]. Both modes can be readily destabilized by the feedback, thereby enabling a large variety of complex dynamics including chaos. Secure communications and RNG have also been demonstrated by use of chaos generated by SRLs with feedback [46]–[50]. Of course, TDS exists in the chaos generated by SRLs, which compromises the performance of these applications, but it can be easily mitigated by appropriately choosing the laser and external parameters. However, the bandwidth is extremely low. Optical injection has also been suggested to improve the chaotic dynamics generated by SRLs, where two different feedback schemes are compared. Nevertheless, the TDS and bandwidth can only be optimized in narrow injection parameter regions, similar to conventional semiconductor lasers. It is expected from the previous research that a cascade-coupling scheme is a cost-effective solution to this problem, but the corresponding study is still missing for these novel SRLs.

In this paper, we study the TDS and bandwidth in three cascade-coupled SRLs, where a master SRL contains optical feedback, the intermediate SRL receives optical injection from the master, and the slave SRL receives optical injection from the intermediate one. The TDS is evaluated by a simple but efficient autocorrelation function (ACF), while the bandwidth is defined as the value for which the range between the DC and the frequency contains 80% of the spectral power. In particular, two different scenarios for TDS concealment and bandwidth are compared and presented in the current study. It is interesting to find simultaneous realization of TDS elimination and bandwidth enhancement over wide regions of the injection strength and the frequency detuning. We further testify the enhanced randomness in the proposed system by carrying out a standard RNG test, thereby confirming its superiority with respect to a single SRL with feedback.

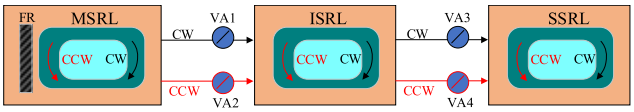

FIGURE 1. Schematic of three cascade-coupled SRLs. MSRL: master SRL. ISRL: intermediate SRL. SSRL: slave SRL. FR: fiber reflector. VA: variable attenuator. CW: clockwise. CCW: counter clockwise.

The remaining of the paper is organized as follows. In Section II, the model of three cascade-coupled SRLs and the corresponding rate equations are introduced in details. Section III is devoted to our main numerical results where TDS and bandwidth are studied in wide injection parameter regions. Finally, a basic conclusion is drawn in Section IV.

II. THEORETICAL MODEL

A. RATE EQUATION MODELS

The architecture of three-cascaded SRLs is shown in Fig.1. It consists of three SRLs, including a master SRL (MSRL), intermediate SRL (ISRL), and slave SRL (SSRL). MSRL is subjected to optical feedback represented by the fiber reflector (FR) in Fig.1, which results in rich nonlinear dynamics in the current system, whereas the other SRLs are subjected unidirectional, optical injection from the adjacent SRL, i.e., from MSRL to ISRL and from ISRL to SSRL. The control parameters are the feedback parameters, the bias current, and the injection parameters. We will mainly focus on the influence of the injection parameters including the injection strength and frequency detuning on the performance of the TDS suppression and bandwidth variation. Note that the injection strength can be easily adjusted by the variable attenuators (VAs) shown in Fig. 1, while the frequency detuning is readily tuned by the temperature controller of each laser, which is not depicted in the figure for the sake of simplicity. The rate equations for the proposed three-cascaded SRLs are written as [49]

$$\frac{dE_M^{cw/ccw}}{dt} = \kappa(1+i\alpha)[gN_M - 1]E_M^{cw/ccw} - k(1-\delta_k)e^{i\phi}E_M^{ccw/cw} + \eta E_M^{cw/ccw}(t-\tau_f)e^{i\theta}, \quad (1)$$

$$\frac{dE_I^{cw/ccw}}{dt} = \kappa(1+i\alpha)[gN_I - 1]E_I^{cw/ccw} - k(1-\delta_k)e^{i\phi}E_I^{ccw/cw} + k_{inj1}E_M^{cw/ccw}(t-\tau_{inj1}) \times \exp(-\omega_1\tau_{inj1} - i2\pi\Delta f_1 t), \quad (2)$$

$$\frac{dE_S^{cw/ccw}}{dt} = \kappa(1+i\alpha)[gN_S - 1]E_S^{cw/ccw} - k(1-\delta_k)e^{i\phi}E_S^{ccw/cw} + k_{inj2}E_I^{cw/ccw}(t-\tau_{inj2}) \times \exp(-\omega_2\tau_{inj2} - i2\pi\Delta f_2 t), \quad (3)$$

TABLE 1. Laser parameter values used in the simulations.

Symbol	Name	Value
α	linewidth-enhancement factor	5
μ	renormalized injection current	2.5
s	self-saturation coefficient	0.005
c	cross-saturation coefficient	0.01
κ	field decay rate	100ns^{-1}
γ_N	carrier decay rate	0.2ns^{-1}
k	backscattering rate	0.44ns^{-1}
δk	asymmetry factor	0.2
ϕ	phase shift	1.5
θ	constant feedback phase	1.5

$$\frac{dN_i^{cw/ccw}}{dt} = \gamma_N[\mu - N_i^{cw/ccw} - g^{cw/ccw}N_i^{cw/ccw}\left|E^{cw/ccw}\right| - g^{ccw/cw}N_i^{cw/ccw}\left|E^{ccw/cw}\right|], \quad (4)$$

$$g_i^{cw/ccw} = 1 - s\left|E_i^{cw/ccw}\right|^2 - c\left|E_i^{ccw/cw}\right|^2 \quad (5)$$

where E(t) is the electric field and N(t) is the carrier density. The subscripts M, I, and S stand for MSRL, ISRL, and SSRL, respectively. The last term in Eq. (1) denotes the optical feedback for MSRL, while the last term in Eqs. (2) and (3) stands for the optical injection from the previous laser, i.e., from MSRL to ISRL and from ISRL to SSRL, respectively. In feedback term, η is the feedback strength, τ_f is the feedback delay time and, θ is the constant feedback phase. In the injection term, k_{inj1} and k_{inj2} are the injection strength, τ_{inj1} and τ_{inj2} represent the injection delay time. As the difference between these lasers is unavoidable in practical situations, we consider the frequency mismatch where, Δf_1 and Δf_2 are the linear frequency detuning between MSRL and ISRL, and between ISRL and SSRL, respectively, with $\omega 1$ and $\omega 2$ being the corresponding angular frequency of MSRL and ISRL. The internal parameters of the three lasers are listed in Table 1, where the definition and value are given.

As mentioned above, we are going to study the chaotic properties of the output generated by a system comprised of three cascade-coupled SRLs. In particular, TDS and bandwidth are two important properties which greatly affect the performance of chaos-based applications, so these will be explored together, aiming at being optimized simultaneously. The commonly used TDS quantifier and effective bandwidth are given below.

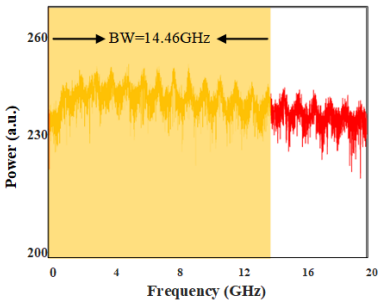

FIGURE 2. A typical example showing the calculated bandwidth in the RF spectrum.

B. TDS QUANTIFIER

TDS is an indicator of the correlation between the time series and its delayed replica at a specific time delay, and can be easily extracted by standard statistical measures, such as, autocorrelation function (ACF) [22]–[25], delayed mutual information (DMI) [23] and permutation entropy (PE) [28], [31]. In the literature, people tended to use two or more of these techniques to show consistent results among them. However, we choose to adopt most common one, ACF, for a TDS measure due to its simplicity and high efficiency. For time series $x(t)$, ACF is defined as

$$C(s) = \frac{< [x(t) - < x(t) >][x_s(t) - < x(t) >] >}{< [x(t) - < x(t) >]^2 >}, \quad (6)$$

where s is the time shift, $< \cdot >$ means the average, and the delayed replica of the original time series has the form of $xs(t) = x(t - s)$.

C. BANDWIDTH

Bandwidth of a chaotic laser system has been extensively studied in many papers due to its importance [30], [43], [52]–[55]. Here we adopt the definition of effective bandwidth, i.e., the bandwidth is defined as the value for which the range between the DC and the frequency contains 80% of the spectral power. For illustrative purposes, Fig. 2 shows an example of the RF spectrum of a laser operating in the fully developed chaotic state, i.e., the so-called coherence collapse. It is worth noting that the bandwidth definition used is only appropriate for the chaotic regime, which has been discussed in [56] and will not be detailed here since it is outside the scope of this article.

III. THEORETICAL RESULTS

In this section, we present the simulation results for TDS and bandwidth of chaos generated by the three lasers. The rate equations given above were integrated by using the forth-order Runge-Kutta algorithm, where the time step was 1ps. We were interested in the chaotic regime, so the corresponding regions were identified. Several measures could be used to distinguish dynamical regions including chaos; see [57] and reference therein. However, the 0-1 test for chaos was employed to identify chaos of interest in this work due to

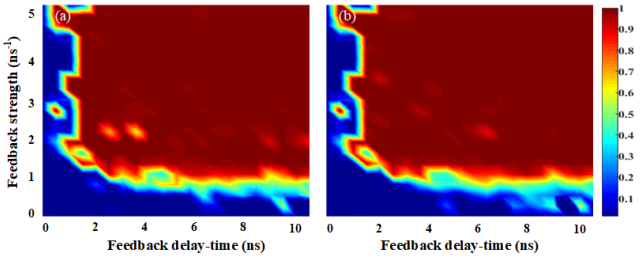

FIGURE 3. The two-dimensional map of the 0-1 test for chaos of MSRL in the (η, τ_f) plane.

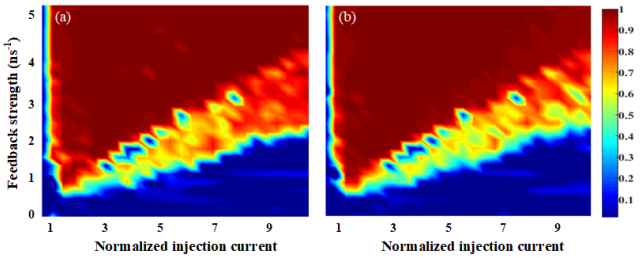

FIGURE 4. The two-dimensional map of the −1 test for chaos of MSRL in the (η, μ) plane.

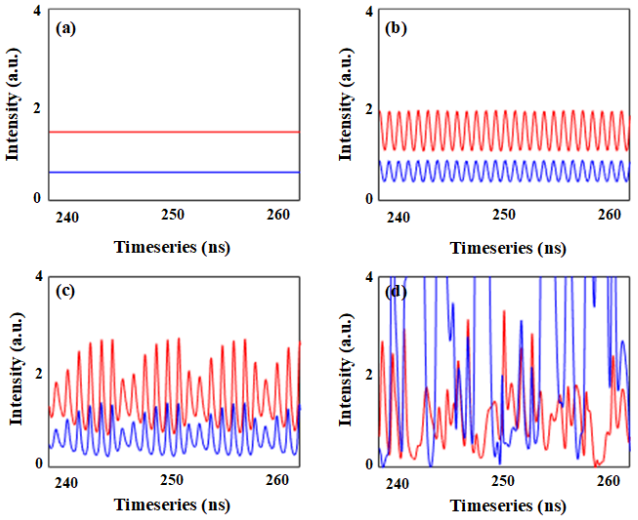

FIGURE 5. Timeseries of the MSRL with different feedback strength, (a) 0.35ns^{-1}, (b) 0.5ns^{-1}, (c) 0.75ns^{-1}, (d) 2.5ns^{-1}. While $\mu = 2.5$, $\tau_f = 6$ns. Red line devotes CW and blue line represents CCW.

its simplicity and accuracy [58]. Especially, '1' stands for chaotic and '0' for nonchaotic states.

A. DYNAMICAL MAPPINGS OF MSRL

The dynamic output of a SRL can be readily steered by varying the feedback parameters and the bias current, which has been numerically demonstrated in the literature. It is of importance to find chaos operation which is a basis of the following study. As, the output of MSRL serves as the input of the cascade configuration, we started by identifying the chaotic regions of MSRL in the above parameter space. Fig. 3 shows the chaotic regions characterized by the 0-1 test for chaos (red) in the plane of the feedback delay and strength. The results for CW and CCW modes are presented, which are almost the same as expected from the model. More importantly, it is interesting to find that MSRL yields chaos over wide regions of the feedback parameters. Similarly, we also studied the influence of the bias current and the injection strength, which is shown in Fig. 4. Again, the results for both modes are included. It can be seen that chaos can be easily obtained by varying these two parameters together although slightly higher feedback strength is required for larger values of the bias current.

As the 0-1 test for chaos only distinguishes chaotic and nonchaotic states, it would be interesting to present temporal traces for various nonlinear dynamics offered by MSRL. As an example, we consider the bias current $\mu = 2.5$ and the feedback delay $\tau_f = 6$ns, and gradually increase the feedback strength eta, which is guided by the two-dimensional colormaps shown in Figs. 3 and 4. The resulting time traces are shown in Fig. 5, where one can clearly observe rich dynamics including continuous-wave, period-one, higher-order periodic and, chaotic states in both CW and CCW modes. Without loss of generality, parameter values $\mu = 2.5$, $\tau_f = 6$ns, and $\eta = 2.5$ns^{-1} are chosen throughout the paper such that chaos operation in MSRL is met.

In the following, we aimed to realize the TDS concealment and bandwidth enhancement in SSRL. For comparison purposes, two cases were considered: Case I for ISRL exhibiting residual TDS, and Case II for no obvious TDS in ISRL.

B. CASE I: ISRL EXHIBITS OBVIOUS TDS

It is known that the optically injected laser shows no obvious TDS only in a narrow region of injection parameters, so it is valuable to check what happens for SSRL when TDS is prominent in ISRL. In this section, the parameter values were chosen such that ISRL exhibits obvious TDS. Fig.6 shows temporal traces, spectra and ACF results, for (a) MSRL, (b) ISRL and (c) SSRL, where parameters used in simulation are $\Delta f_1 = 0$GHz, $k_{inj1} = 35$ns^{-1}, $\Delta f_2 = 20$GHz, and $k_{inj2} = 65$ns^{-1}. The time series and the corresponding RF spectra confirm chaos operation in the three lasers. It can be seen that ISRL's bandwidth is similar to that of MSRL due to the injection-locking effect, which also results in obvious TDS in SRL. By contrast, SSRL exhibits broad bandwidth and well suppressed TDS which benefits from the cascade-injection scenario. Besides, CW and CCW display consistent features for bandwidth and ACF, which can be expected from the laser ring architecture.

We were interested to know the chaotic regions of SSRL in the (k_{inj2}, Δf_2)-plane. To this end, the widely used 0-1 test for chaos was adopted here. Fig.7 shows the corresponding results. As can be seen, chaos operation is seen for SSRL when the injection strength exceeds a threshold value $k_{inj2} \approx 10$ns^{-1}, where optical injection takes effect. This is expected since the driving signal from ISRL is chaotic.

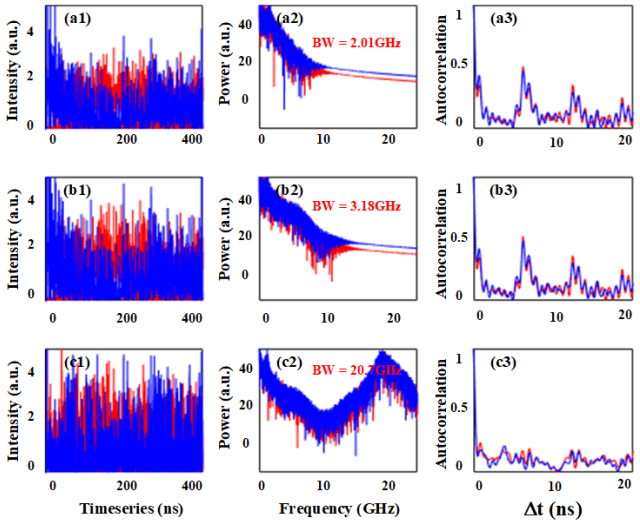

FIGURE 6. The timeseries (a1-c1), power spectrum (a2-c2) and ACF (a3-c3) of the MSRL (a1-a3), ISRL (b1-b3) and SSRL (c1-c3), respectively. The parameters are set as: $\Delta f_1 = 0$GHz, $k_{inj1} = 35\text{ns}^{-1}$, $\Delta f_2 = 20$GHz, $k_{inj2} = 65\text{ns}^{1}$.

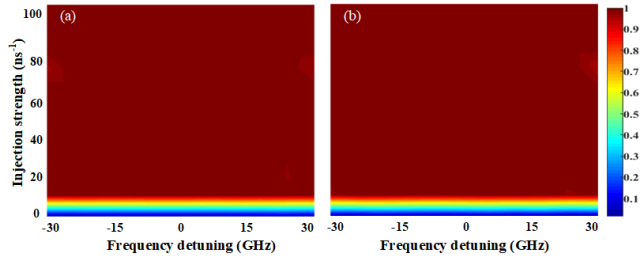

FIGURE 7. The 0-1 test for chaos of SSRL under the condition of Case I. The parameters are set as: $\Delta f_1 = 0$GHz, $k_{inj1} = 35\text{ns}^{-1}$.

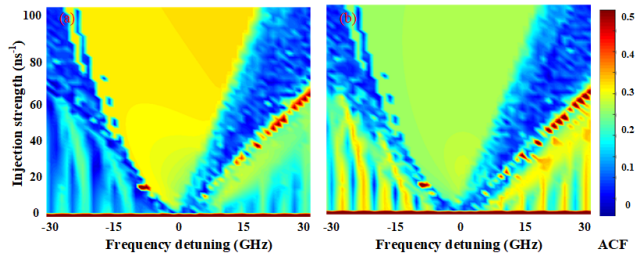

FIGURE 8. Two-D map of TDS value of SSRL in the parameter plane (k_{inj2}, Δf_2) while $\Delta f_1 = 0$GHz, $k_{inj1} = 35\text{ns}^{-1}$.

We further studied the effects of injection parameters (k_{inj2}, $\Delta f2$) on the TDS and bandwidth of SSRL, and the results are shown in Figs.8 and 9, respectively. Outside the injection locking region, it is possible to cancel TDS and enhance bandwidth in SSRL at the same time, as can be seen from both figures. However, such region for achieving both goals is narrow, which confirms previous observations in cascaded-coupled systems consisting of conventional EELs [35] or VCSELs [34].

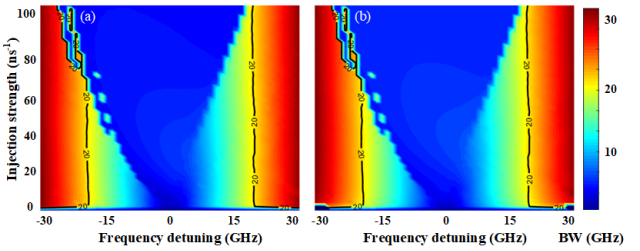

FIGURE 9. Two-D map of bandwidth value of SSRL in the parameter plane (k_{inj2}, Δf_2) while $\Delta f_1 = 0$GHz, $k_{inj1} = 35\text{ns}^{-1}$.

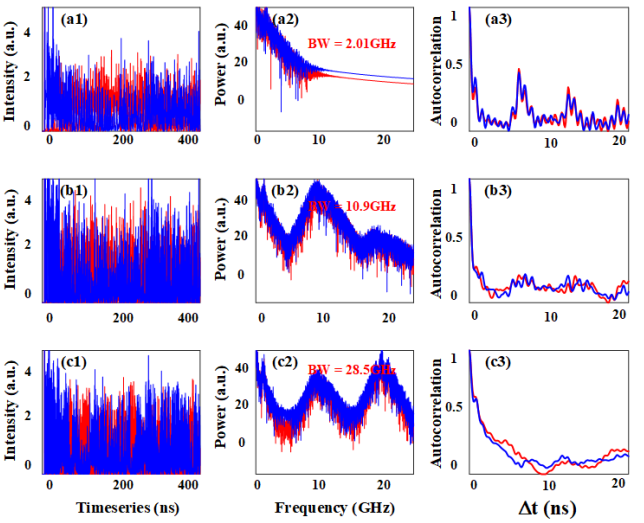

FIGURE 10. The timeseries (a1-c1), power spectrum (a2-c2) and ACF (a3-c3) of the MSRL (a1-a3), ISRL (b1-b3) and SSRL (c1-c3), respectively. The parameters are set as: $\Delta f_1 = 10$GHz, $k_{inj1} = 35\text{ns}^{-1}$, $\Delta f_2 = 20$GHz, $k_{inj2} = 65\text{ns}^{1}$.

C. CASE II: ISRL EXHIBITS NO OBVIOUS TDS

In fact, one can find narrow regions where ISRL has no obvious TDS as mentioned above. The injection parameters $k_{inj1} = 35\text{ns}^{-1}$ and $\Delta f_1 = 10$GHzare chosen such that such requirement is met. Fig. 10 displays the corresponding results, where $k_{inj2} = 65\text{ns}^{-1}$ and $\Delta f_2 = 20$GHz.It is interesting to find that TDS can be cancelled in both ISRL and SSRL, and bandwidth is enhanced simultaneously, different from the case shown in Fig. 6.

Again, the 0-1 test for chaos was used for confirming chaos operation in SSRL and the results are shown in Fig. 11. Similar to Case I depicted in Fig. 7, chaotic states are guaranteed almost in the whole region, which gives us confidence that we are dealing with chaotic signals in the following study.

Figure 12 shows the two-dimensional TDS maps of SSRL in the plane of injection strength k_{inj2} against frequency detuning Δf_2. Almost in the whole region, the TDS is limited to a small value, i.e., below ∼0.1, which means that TDS is almost completely cancelled. In fact, this is expected since autocorrelation property in the driving signal from SSRL has already been well suppressed. In the same parameter space, the bandwidth was calculated for SSRL. As can be seen from Fig. 13, bandwidth enhancement is achieved in

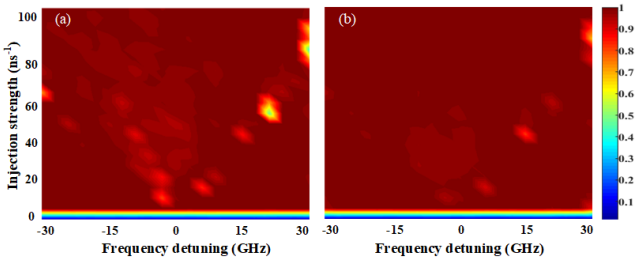

FIGURE 11. The 0-1 test for chaos of SSRL under the condition of Case II.

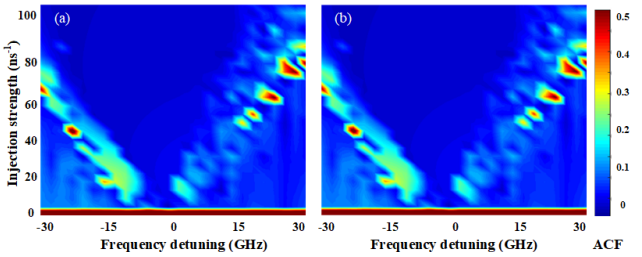

FIGURE 12. Two-D map of TDS value of SSRL in the parameter plane (k_{inj2}, Δf_2) under the condition of Case II. The parameters are set as: $\Delta f_1 = 10$GHz, $k_{inj1} = 35$ns^{-1}.

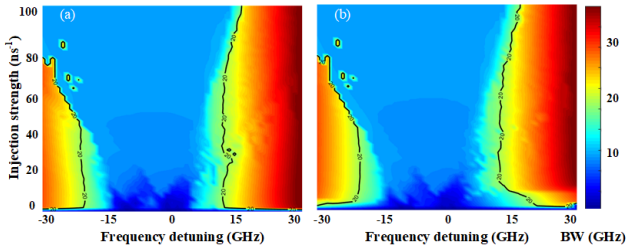

FIGURE 13. Two-D map of bandwidth value of SSRL in the parameter plane (k_{inj2}, Δf_2) under the condition of Case II. The parameters are set as: $\Delta f_1 = 10$GHz, $k_{inj1} = 35$ns^{-1}.

red regions similar to Fig. 9. This is because the bandwidth is almost determined by the frequency detuning when the difference of two lasers' frequencies is large. Combining results in Figs. 12 and 13 indicates that simultaneous TDS concealment and bandwidth enhancement is realized in the red region of Fig. 13 where bandwidth is large. In this sense, one can achieve these two goals in wider regions compared to Case I shown in Figs. 8 and 9.

D. POTENTIAL BENEFIT OF IMPROVED CHAOTIC DYNAMICS

TDS cancellation and bandwidth enhancement are important for chaos-base applications. Therefore, we would like to carry out a proof-of-concept randomness test in order to demonstrate the importance and significance of the current work on the improvement of chaotic dynamics using the cascaded-coupling scheme.

As an example, we considered the parameters used for Fig. 6(c) and the generated chaotic signals in SSRL were used as the random entropy. A multibit extraction scheme

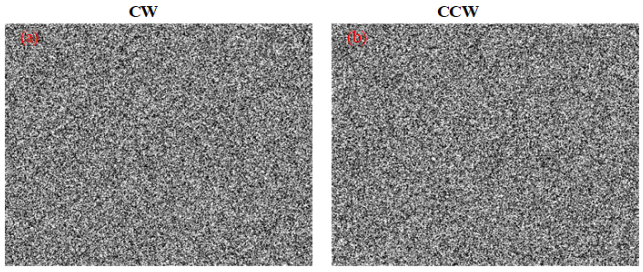

FIGURE 14. Random bit patterns in a two-dimensional plane. Bits 1 and 0 are converted to white and black dots, respectively, and placed from left- to right-hand sides (and from top to bottom).

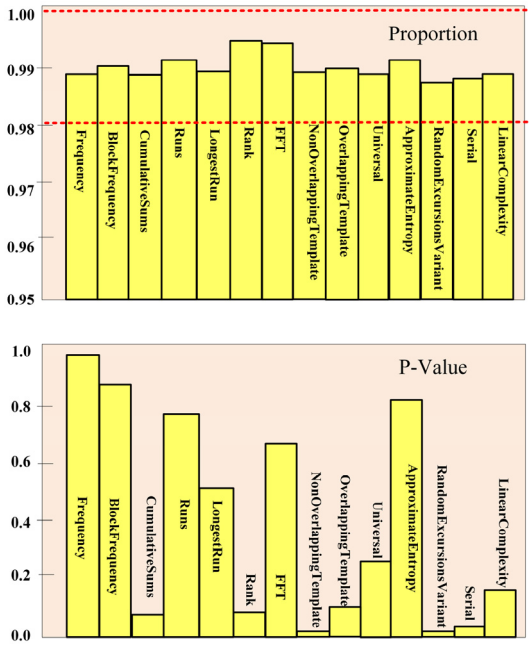

FIGURE 15. Result of NIST statistical tests for physical random bits. The results have been performed using 1000 samples of 1Mbit and a significance level $\alpha = 1$, for "Success", the P-value should be larger than 0.0001 and the proportion should be in the 0.99 ± 0.0094392 range. For the tests that produce multiple P values and proportions, the worst case is shown.

was employed for generating bit sequences and XOR-post-processing technique was used for killing the bias. We found that 5 least significant bits per sample could be kept for concatenating bit sequences, which could pass widely used NIST suite for randomness test.

Figure 14 shows the two-dimensional map of the generated random bit patterns. It can be seen clearly that white and black dots representing bits "0" and "1" distribute uniformly and irregularly for CW and CCW cases. This confirms qualitatively the high randomness for the generated bits. Then NIST suite was used to measure randomness quantitatively. The results for Proportion and P-value are presented in Fig. 15. From this figure, one can see that both of them are limited to the required interval, i.e., the minimum proportion is above the threshold of 0.9805608 while the minimum of the calculated P-values is greater than 0.0001. This indicates that the

generated bit sequences pass NIST tests with only minimum post processing.

IV. CONCLUSION

In this paper, we have numerically investigated the TDS concealment and bandwidth enhancement in three-cascaded SRLs, where MSRL is subjected to optical feedback, ISRL is subjected to optical injection from MSRL, and SSRL is subjected to optical injection from ISRL. We have compared two scenarios including ISRL with or without obvious TDS and found distinct features in the two cases. We have found that the proposed scheme allows for TDS enhancement and bandwidth enhancement over wide regions of control parameters. Moreover, we have numerically demonstrated that the generated bit sequences from the enhanced chaotic dynamics could pass the standard randomness test after minimum post processing. Our study confirms that SRL's dynamics could be greatly enhanced by employing the cascade-coupling scheme and it could serve important sources for chaos-based applications.

REFERENCES

[1] A. Argyris *et al.*, "Chaos-based communications at high bit rates using commercial fibre-optic links," *Nature*, vol. 438, pp. 343–346, Nov. 2005.

[2] N. Li, H. Susanto, B. Cemlyn, I. D. Henning, and M. J. Adams, "Secure communication systems based on chaos in optically pumped spin-VCSELs," *Opt. Lett.*, vol. 42, no. 17, pp. 3494–3497, Sep. 2017.

[3] N. Li, W. Pan, L. Yan, B. Luo, X. Zou, and S. Xiang, "Enhanced two-channel optical chaotic communication using isochronous synchronization," *IEEE J. Sel. Topics Quantum Electron.*, vol. 19, no. 4, Aug. 2013, Art. no. 0600109.

[4] J. R. Terry and G. D. VanWiggeren, "Chaotic communication using generalized synchronization," *Chaos, Solitons Fractals*, vol. 12, no. 1, pp. 145–152, Jan. 2001.

[5] N. Jiang, C. Xue, Y. Lv, and K. Qiu, "Physically enhanced secure wavelength division multiplexing chaos communication using multimode semiconductor lasers," *Nonlinear Dyn.*, vol. 86, no. 3, pp. 1937–1949, Aug. 2016.

[6] A. Uchida *et al.*, "Fast physical random bit generation with chaotic semiconductor lasers," *Nature Photon.*, vol. 2, no. 12, pp. 728–732, 2008.

[7] I. Reidler, Y. Aviad, M. Rosenbluh, and I. Kanter, "Ultrahigh-speed random number generation based on a chaotic semiconductor laser," *Phys. Rev. Lett.*, vol. 103, no. 2, Jul. 2009, Art. no. 024102.

[8] P. Li *et al.*, "Fully photonics-based physical random bit generator," *Opt. Lett.*, vol. 41, no. 14, pp. 3347–3350, Jul. 2016.

[9] N. Li *et al.*, "Two approaches for ultrafast random bit generation based on the chaotic dynamics of a semiconductor laser," *Opt. Express*, vol. 22, no. 6, pp. 6634–6646, Mar. 2014.

[10] D. Rontani, D. Choi, C.-Y. Chang, A. Locquet, and D. S. Citrin, "Compressive sensing with optical chaos," *Sci. Rep.*, vol. 6, Dec. 2016, Art. no. 35206.

[11] S. Xiang, Y. Zhang, X. Guo, A. Wen, and Y. Hao, "Photonic generation of neuron-like dynamics using VCSELs subject to double polarized optical injection," *J. Lightw. Technol.*, vol. 36, no. 19, pp. 4227–4234, Oct. 1, 2018.

[12] S. Y. Xiang *et al.*, "Cascadable neuron-Like spiking dynamics in coupled VCSELs subject to orthogonally polarized optical pulse injection," *IEEE J. Sel. Topics Quantum Electron.*, vol. 23, no. 6, Nov. 2017, Art. no. 1700207.

[13] L. Larger *et al.*, "Photonic information processing beyond Turing: An optoelectronic implementation of reservoir computing," *Opt. Express*, vol. 20, no. 3, pp. 3241–3249, 2012.

[14] F.-Y. Lin and J.-M. Liu, "Chaotic lidar," *IEEE J. Sel. Topics Quantum Electron.*, vol. 10, no. 5, pp. 991–997, Sep./Oct. 2004.

[15] M. Sciamanna and K. A. Shore, "Physics and applications of laser diode chaos," *Nature Photon.*, vol. 9, pp. 151–162, Feb. 2015.

[16] G.-Q. Xia, S.-C. Chan, and J.-M. Liu, "Multistability in a semiconductor laser with optoelectronic feedback," *Opt. Express*, vol. 15, no. 2, pp. 572–576, Feb. 2007.

[17] C.-H. Lee and S.-Y. Shin, "Self-pulsing, spectral bistability, and chaos in a semiconductor laser diode with optoelectronic feedback," *Appl. Phys. Lett.*, vol. 62, no. 9, pp. 922–924, Apr. 1993.

[18] I. Gatare, J. Buesa, H. Thienpont, K. Panajotov, and M. Sciamanna, "Polarization switching bistability and dynamics in vertical-cavity surface-emitting laser under orthogonal optical injection," *Opt. Quantum Electron.*, vol. 38, nos. 4–6, pp. 429–443, Jan. 2006.

[19] F.-Y. Lin and J.-M. Liu, "Nonlinear dynamics of a semiconductor laser with delayed negative optoelectronic feedback," *IEEE J. Quantum Electron.*, vol. 39, no. 4, pp. 562–568, Apr. 2003.

[20] M. Cheng, L. Deng, H. Li, and D. Liu, "Enhanced secure strategy for electro-optic chaotic systems with delayed dynamics by using fractional Fourier transformation," *Opt. Express*, vol. 22, no. 5, pp. 5241–5251, Mar. 2014.

[21] R. Hegger, M. J. Bünner, H. Kantz, and A. Giaquinta, "Identifying and modeling delay feedback systems," *Phys. Rev. Lett.*, vol. 81, no. 3, pp. 558–561, Jul. 1998.

[22] R. M. Nguimdo, M. C. Soriano, and P. Colet, "Role of the phase in the identification of delay time in semiconductor lasers with optical feedback," *Opt. Lett.*, vol. 36, no. 22, pp. 4332–4334, Nov. 2011.

[23] D. Rontani, A. Locquet, M. Sciamanna, D. S. Citrin, and S. Ortin, "Time-delay identification in a chaotic semiconductor laser with optical feedback: A dynamical point of view," *IEEE J. Quantum Electron.*, vol. 45, no. 7, pp. 879–891, Jul. 2009.

[24] R. M. Nguimdo, P. Colet, L. Larger, and L. Pesquera, "Digital key for chaos communication performing time delay concealment," *Phys. Rev. Lett.*, vol. 107, Jul. 2011, Art. no. 034103.

[25] D. Rontani, A. Locquet, M. Sciamanna, and D. S. Citrin, "Loss of time-delay signature in the chaotic output of a semiconductor laser with optical feedback," *Opt. Lett.*, vol. 32, no. 20, pp. 2960–2962, 2007.

[26] J. G. Wu, G. Q. Xia, and Z. M. Wu, "Suppression of time delay signatures of chaotic output in a semiconductor laser with double optical feedback," *Opt. Express*, vol. 17, no. 22, pp. 20124–20133, 2009.

[27] Z.-Q. Zhong, Z.-M. Wu, and G.-Q. Xia, "Experimental investigation on the time-delay signature of chaotic output from a 1550 nm VCSEL subject to FBG feedback," *Photon. Res.*, vol. 5, no. 1, pp. 6–10, Feb. 2017.

[28] S. Priyadarshi, Y. Hong, I. Pierce, and K. A. Shore, "Experimental investigations of time-delay signature concealment in chaotic external cavity VCSELs subject to variable optical polarization angle of feedback," *IEEE J. Sel. Topics Quantum Electron.*, vol. 19, no. 4, Jan. 2013, Art. no. 1700707.

[29] N. Li, W. Pan, A. Locquet, and D. S. Citrin, "Time-delay concealment and complexity enhancement of an external-cavity laser through optical injection," *Opt. Lett.*, vol. 40, no. 19, pp. 4416–4419, Sep. 2015.

[30] N. Li *et al.*, "Photonic generation of wideband time-delay-signature-eliminated chaotic signals utilizing an optically injected semiconductor laser," *IEEE J. Quantum Electron.*, vol. 48, no. 10, pp. 1339–1345, Oct. 2012.

[31] Y. Hong, "Experimental study of time-delay signature of chaos in mutually coupled vertical-cavity surface-emitting lasers subject to polarization optical injection," *Opt. Express*, vol. 21, no. 15, pp. 17894–17903, 2013.

[32] J. G. Wu, Z. M. Wu, G. Q. Xia, and G. Y. Feng, "Evolution of time delay signature of chaos generated in a mutually delay-coupled semiconductor lasers system," *Opt. Exp.*, vol. 20, no. 2, pp. 1741–1753, Jan. 2012.

[33] P. Mu, W. Pan, L. Yan, B. Luo, N. Li, and M. Xu, "Experimental evidence of time-delay concealment in a DFB laser with dual-chaotic optical injections," *IEEE Photon. Technol. Lett.*, vol. 28, no. 2, pp. 131–134, Jan. 15, 2016.

[34] Y. Hong, A. Quirce, B. Wang, S. Ji, K. Panajotov, and P. S. Spencer, "Concealment of chaos time-delay signature in three-cascaded vertical-cavity surface-emitting lasers," *IEEE J. Quantum Electron.*, vol. 52, no. 8, Aug. 2016, Art. no. 2400508.

[35] N. Li, W. Pan, S. Xiang, L. Yan, B. Luo, and X. Zou, "Loss of time delay signature in broadband cascade-coupled semiconductor lasers," *IEEE Photon. Technol. Lett.*, vol. 24, no. 23, pp. 2187–2190, Dec. 1, 2012.

[36] S. Sivaprakasam and K. A. Shore, "Cascaded synchronization of external-cavity laser diodes," *Opt. Lett.*, vol. 26, no. 5, pp. 253–255, Mar. 2001.

[37] M. W. Lee, J. Paul, C. Masoller, and K. A. Shore, "Observation of cascade complete-chaos synchronization with zero time lag in laser diodes," *J. Opt. Soc. Amer. B, Opt. Phys.*, vol. 23, no. 5, pp. 846–851, May 2006.

[38] R. Sakuraba, K. Iwakawa, K. Kanno, and A. Uchida, "Tb/s physical random bit generation with bandwidth-enhanced chaos in three-cascaded semiconductor lasers," *Opt. Express*, vol. 23, no. 2, pp. 1470–1490, Jan. 2015.
[39] Y. Xu, L. Zhang, P. Lu, S. Mihailov, L. Chen, and X. Bao, "Time-delay signature concealed broadband gain-coupled chaotic laser with fiber random grating induced distributed feedback," *Opt. Laser Technol.*, vol. 109, pp. 654–658, Jan. 2019.
[40] J. Zhang, M. Li, A. Wang, M. Zhang, Y. Ji, and Y. Wang, "Time-delay-signature-suppressed broadband chaos generated by scattering feedback and optical injection," *Appl. Opt.*, vol. 57, no. 22, pp. 6314–6317, Aug. 2018.
[41] N. Jiang *et al.*, "Generation of broadband chaos with perfect time delay signature suppression by using self-phase-modulated feedback and a microsphere resonator," *Opt. Lett.*, vol. 43, no. 21, pp. 5359–5362, Nov. 2018.
[42] S.-S. Li, X.-Z. Li, and S.-C. Chan, "Chaotic time-delay signature suppression with bandwidth broadening by fiber propagation," *Opt. Lett.*, vol. 43, no. 19, pp. 4751–4754, Oct. 2018.
[43] A. Wang, B. Wang, L. Li, Y. Wang, and K. A. Shore, "Optical heterodyne generation of high-dimensional and broadband white chaos," *IEEE J. Sel. Topics Quantum Electron.*, vol. 21, no. 6, Nov. 2015, Art. no. 1800710.
[44] C.-H. Cheng, Y.-C. Chen, and F.-Y. Lin, "Chaos time delay signature suppression and bandwidth enhancement by electrical heterodyning," *Opt. Express*, vol. 23, no. 3, pp. 2308–2319, Feb. 2015.
[45] C. Born, G. Yuan, Z. Wang, and S. Yu, "Nonlinear gain in semiconductor ring lasers," *IEEE J. Quantum Electron.*, vol. 44, no. 11, pp. 1055–1064, Nov. 2008.
[46] G. Friart, G. Van der Sande, M. Khoder, T. Erneux, and G. Verschaffelt, "Stability of steady and periodic states through the bifurcation bridge mechanism in semiconductor ring lasers subject to optical feedback," *Opt. Express*, vol. 25, no. 1, pp. 339–350, Jan. 2017.
[47] S.-S. Li, X.-Z. Li, J.-P. Zhuang, G. Mezosi, M. Sorel, and S.-C. Chan, "Square-wave oscillations in a semiconductor ring laser subject to counter-directional delayed mutual feedback," *Opt. Lett.*, vol. 41, no. 4, pp. 812–815, Feb. 2015.
[48] S.-S. Li, V. Pusino, S.-C. Chan, and M. Sorel, "Experimental investigation on feedback insensitivity in semiconductor ring lasers," *Opt. Lett.*, vol. 43, no. 9, pp. 1974–1977, May 2018.
[49] N. Li, R. M. Nguimdo, A. Locquet, and D. S. Citrin, "Enhancing optical-feedback-induced chaotic dynamics in semiconductor ring lasers via optical injection," *Nonlinear Dyn.*, vol. 92, no. 2, pp. 315–324, Jan. 2018.
[50] M. Khoder, G. Van der Sande, and G. Verschaffelt, "Reducing the sensitivity of semiconductor ring lasers to external optical injection using selective optical feedback," *J. Appl. Phys.*, vol. 124, no. 13, 2018, Art. no. 133101.
[51] T. T. M. van Schaijk, D. Lenstra, E. A. J. M. Bente, and K. A. Williams, "Rate-equation theory of a feedback insensitive unidirectional semiconductor ring laser," *Opt. Express*, vol. 26, no. 10, pp. 13361–13369, May 2018.
[52] A. Wang, Y. Yang, B. Wang, B. Zhang, L. Li, and Y. Wang, "Generation of wideband chaos with suppressed time-delay signature by delayed self-interference," *Opt. Express*, vol. 21, no. 7, pp. 8701–8710, Apr. 2013.
[53] S. Y. Xiang *et al.*, "Wideband unpredictability-enhanced chaotic semiconductor lasers with dual-chaotic optical injections," *IEEE J. Quantum Electron.*, vol. 48, no. 8, pp. 1069–1076, Aug. 2012.
[54] A. Uchida, T. Heil, Y. Liu, P. Davis, and T. Aida, "High-frequency broadband signal generation using a semiconductor laser with a chaotic optical injection," *IEEE J. Quantum Electron.*, vol. 39, no. 11, pp. 1462–1467, Nov. 2003.
[55] Y. Takiguchi, K. Ohyagi, and J. Ohtsubo, "Bandwidth-enhanced chaos synchronization in strongly injection-locked semiconductor lasers with optical feedback," *Opt. Lett.*, vol. 28, no. 5, pp. 319–321, Apr. 2003.
[56] F. Y. Lin, Y. K. Chao, and T. C. Wu, "Effective bandwidths of broadband chaotic signals," *IEEE J. Quantum Electron.*, vol. 48, no. 8, pp. 1010–1014, Aug. 2012.
[57] N. Li, H. Susanto, B. R. Cemlyn, I. D. Henning, and M. J. Adams, "Stability and bifurcation analysis of spin-polarized vertical-cavity surface-emitting lasers," *Phys. Rev. A, Gen. Phys.*, vol. 96, no. 1, Jul. 2017, Art. no. 013840.
[58] G. A. Gottwald and I. Melbourne, "On the implementation of the 0–1 test for chaos," *SIAM J. Appl. Dyn. Syst.*, vol. 8, no. 1, pp. 129–145, Jun. 2009.

PENGHUA MU (M'18) received the B.S. degree in communication engineering and the Ph.D. degree in optoelectronics from Southwest Jiaotong University, China, in 2009 and 2016, respectively. He joined the Institute of Science and Technology for Opto-electronic Information, Yantai University. His current research interests include nonlinear dynamic of semiconductor lasers, random number generation, and chaotic security communication.

PENGFEI HE received the Ph.D. degree in electromagnetic field and microwave technology from the Beijing University of Posts and Telecommunications, in 2007. He joined the Institute of Science and Technology for Opto-electronic Information, Yantai University, where he is currently an Associate Professor.

He has published more than 30 high-quality academic papers in the aspect of UWB communication, cognitive radio, and wireless sensor network. His current research interests include short-range wireless communication technology, wireless body area networks, broadband access networks, and electromagnetic compatibility.

NIANQIANG LI (M'17) received the B.S. degree in communication engineering and the Ph.D. degree in optoelectronics from Southwest Jiaotong University, China, in 2008 and 2016, respectively. His thesis work concerned nonlinear dynamics of semiconductor lasers and its applications to secure communications and random number generation.

From 2013 to 2014, he was a Visiting Scholar with the Georgia Institute of Technology (Georgia Tech), USA. From 2016 to 2018, he was with the School of Computer Science and Electronic Engineering, University of Essex, as a Postdoctoral Researcher focusing on a collaborative EPSRC-funded project in U.K. Since 2018, he has been with the School of Electrical Engineering and Computer Science, University of Ottawa, Canada, working on microwave photonics. He has authored or co-authored more than 60 peer-reviewed journal papers. His current research mainly focuses on the area of the laser dynamics, chaos-based communication and random number generation, and microwave photonics. He is an Associate Editor of the IEEE ACCESS.